PAIN

CDK5 inhibits the clathrin-dependent internalization of TRPV1 by phosphorylating the clathrin adaptor protein AP2μ2

Jiao Liu[1,2]*, Junxia Du[3]*, Yun Wang[2,4]†

Transient receptor potential vanilloid 1 (TRPV1), a nonselective, ligand-gated cation channel, responds to multiple noxious stimuli and is targeted by many kinases that influence its trafficking and activity. Studies on the internalization of TRPV1 have mainly focused on that induced by capsaicin or other agonists. Here, we report that constitutive internalization of TRPV1 occurred in a manner dependent on clathrin, dynamin, and adaptor protein complex 2 (AP2). The μ2 subunit of AP2 (AP2μ2) interacted directly with TRPV1 and was required for its constitutive internalization. Cyclin-dependent kinase 5 (CDK5) phosphorylated AP2μ2 at Ser[45], which reduced the interaction between TRPV1 and AP2μ2, leading to decreased TRPV1 internalization. Intrathecal delivery of a cell-penetrating fusion peptide corresponding to the Cdk5 phosphorylation site in AP2μ2, which competed with AP2μ2 for phosphorylation by Cdk5, increased the abundance of TRPV1 on the surface of dorsal root ganglion neurons and reduced complete Freund's adjuvant (CFA)–induced inflammatory thermal hyperalgesia in rats. In addition to describing a mechanism of TRPV1 constitutive internalization and its inhibition by CDK5, these findings demonstrate that CDK5 promotes inflammatory thermal hyperalgesia by reducing TRPV1 internalization, providing previously unidentified insights into the search for drug targets to treat pain.

INTRODUCTION

Transient receptor potential (TRP) channels are a large family of cation channels involved in diverse physiological functions and are present in almost all cell types. They play important roles, ranging from Ca^{2+} absorption, vasorelaxation, cell death, mechanotransduction, and hearing to the mediation of pH, heat, taste, osmolarity, and pain sensations (*1*). Dysfunctions of TRP channels have been linked to several diseases (*2*). TRP vanilloid 1 (TRPV1), which is highly abundant on medium- and small-diameter nociceptive neurons, is a nonselective, ligand-gated cation channel that contributes to the development of diverse types of pain such as inflammatory pain, bone cancer pain, migraine, irritable bowel syndrome, and arthritis (*3*, *4*). TRPV1 also plays important roles in many other physiological and pathological processes such as itch, metabolic decline, autoimmune diabetes, pancreatitis, and modulation of vascular function (*5*–*9*).

Various kinases regulate the functions of TRPV1 by phosphorylation, which changes the functional characteristics of the channel or influences the trafficking of the channel, leading to the redistribution of surface TRPV1 (*10*–*14*). TRPV1 desensitization is usually Ca^{2+} dependent and coupled to various downstream signaling proteins and physiological activities (*6*, *15*–*18*). Our previous studies have shown that phosphorylation at Thr^{406} in rat TRPV1 (corresponding to Thr^{407} in human TRPV1) by cyclin-dependent kinase 5 (CDK5) can increase the surface distribution of TRPV1 (*19*). In addition, we have demonstrated that CDK5 promotes the interaction between the kinesin motor protein KIF13B and TRPV1 by phosphorylating KIF13B, which leads to an increase in surface TRPV1 and promotes inflammatory thermal hyperalgesia (*20*).

Clathrin-mediated endocytosis is the major route of receptor internalization at the plasma membrane. The major clathrin adaptor at the plasma membrane is the adaptor protein 2 (AP2) complex of four adaptins, which undergoes several large-scale conformational changes to bind to the membrane, recognize cargo, recruit clathrin to the plasma membrane, and promote the assembly of a polygonal clathrin lattice that leads to the formation of clathrin-coated endocytic vesicles (*21*–*23*). Dynamin is involved in a broad spectrum of endocytic events (*24*–*26*) because it facilitates the endocytic process by promoting membrane invagination and fission of cargo-bearing clathrin-coated vesicles from the plasma membrane.

The trafficking of ion channel proteins to the cell membrane and their internalization are in dynamic equilibrium. However, the mechanism of TRPV1 internalization has not yet been fully revealed. TRPV1 internalization was first observed by the Planells-Cases team when they were studying the desensitization effect of GABARAP (γ-aminobutyric acid receptor–related protein) on TRPV1 (*15*). Scholich's team subsequently found that the E3 ubiquitin ligase Myc-binding protein 2 (MYCBP2) could promote the internalization of TRPV1 by inhibiting the p38 mitogen-activate protein kinase signaling pathway (*27*). At present, research on the internalization of TRPV1 has mainly focused on capsaicin or resiniferatoxin and other agonists that induce internalization. Few studies have addressed the mechanism of constitutive internalization under basal physiological conditions. The constitutive internalization of channel proteins contributes to maintenance of the stability of membrane surface protein distribution, which is important for channel function. Here, we show that TRPV1 internalization occurred in a clathrin-dependent manner and was negatively regulated by CDK5. Interfering with Cdk5-induced inhibition of TRPV1 internalization reduced inflammatory thermal hyperalgesia, suggesting potential drug targets for the clinical treatment of pain.

[1]Center of Medical and Health Analysis, Peking University Health Science Center, Beijing 100191, China. [2]Neuroscience Research Institute and Department of Neurobiology, School of Basic Medical Sciences, the Key Laboratory for Neuroscience of the Ministry of Education/National Health Commission and State Key Laboratory of Natural and Biomimetic Drugs, Peking University, Beijing 100191, China. [3]College of Biological Science and Engineering, Xingtai University, Xingtai 054001, Hebei Province, China. [4]PKU-IDG/McGovern Institute for Brain Research, Peking University, Beijing 100871, China.
*These authors contributed equally to this work.
†Corresponding author. Email: wangy66@bjmu.edu.cn

RESULTS

TRPV1 is constitutively internalized under basal conditions

Both constitutive and ligand-induced internalization are important for the regulation of ion channels. Constitutive internalization occurs under basal conditions and contributes to the dynamic recycling of membrane proteins in both the basal physiological and stimulated states (*28*, *29*). To investigate whether TRPV1 was internalized under basal conditions, we performed biotinylation internalization assays. Surface proteins on human embryonic kidney (HEK) 293 cells expressing enhanced green fluorescent protein (EGFP)–tagged TRPV1 (EGFP-TRPV1) were biotinylated, and then the cells were incubated for various amounts of time to allow biotinylated proteins to be internalized. The remaining surface biotinylation was removed, and internalized biotinylated proteins were purified from cell lysates and analyzed by Western blotting (Fig. 1A). EGFP-tagged TRPV1 was internalized in HEK293 cells, and there was no significant difference between the amount of EGFP-TRPV1 internalized in 10 min versus 30 min (Fig. 1B), indicating that internalization was a dynamically balanced process. To determine whether endogenous TRPV1 was internalized, we also subjected cultured primary rat dorsal root ganglion (DRG) neurons to an antibody-feeding experiment with a fluorescein isothiocyanate (FITC)–conjugated antibody recognizing the extracellular domain of TRPV1 (Fig. 1C). Whereas the green fluorescent particles were found mostly on the surface of control cells that were fed the antibodies at 4°C, some were located within cells that were fed the antibodies at 37°C (Fig. 1D). Together, these results show that both exogenous and endogenous TRPV1 were internalized under basal conditions. Because membrane trafficking of protein channels usually modulates their physiological function (*28*), we tested whether blocking internalization reduced the cellular response to TRPV1 stimulation. We performed Fluo-4 AM (acetyloxymethyl ester, a cell-permeant chelator) Ca^{2+} imaging with both HEK293 cells and DRG neurons stimulated with capsaicin after preincubation of the cells at 4°C (basal internalization reduced) or 37°C (basal internalization maintained). Capsaicin evoked a rapid, robust increase in intracellular Ca^{2+} concentration in cells pretreated at 4°C but a smaller increase in intracellular Ca^{2+} concentration in cells pretreated at 37°C (Fig. 1, E and F), suggesting that constitutive internalization reduces TRPV1 channel membrane function.

TRPV1 internalization depends on clathrin and dynamin

Clathrin-mediated endocytosis is the major mechanism by which integral membrane proteins are internalized and delivered to endosomes for subsequent degradation or recycling back to the cell surface. Clathrin-mediated endocytosis is a highly orchestrated process involving many proteins that recruit and concentrate cargo at specific membrane domains, followed by clathrin coat building, and, finally, dynamin-mediated scission of the fully formed clathrin-coated vesicle from the plasma membrane (*30*). Internalization of the TRP family member TRPV5 has been reported to occur in a clathrin- and dynamin-dependent manner (*31*). To investigate the mechanism of TRPV1 internalization, we inhibited clathrin-dependent internalization by treating the cells with a hypertonic solution, which prevents the formation of clathrin pits (*32*). We observed a clear decrease in TRPV1 internalization in the cells treated with hypertonic solution compared to control cells treated with phosphate-buffered saline (PBS) (Fig. 2A). The TFR, which is known to be internalized through a clathrin-dependent pathway, was used as a positive control. TRPV1 and clathrin also colocalized in HEK293 cells as determined by immunofluorescence (Fig. 2B). We also performed biotinylation assays in EGFP-TRPV1–expressing HEK293 cells, in which clathrin-mediated endocytosis was compromised (Fig. 2C). Knockdown of CHC using small interfering RNAs (siRNAs), which reduces the abundance of endogenous clathrin (*24*), increased the surface abundance of TRPV1 compared with nonsilenced control cells (Fig. 2D). During clathrin-dependent internalization, dynamin plays a key role in separating the clathrin-coated vesicle from the cell membrane. To investigate the effect of dynamin on clathrin-dependent internalization of TRPV1, we performed the biotinylation assay in EGFP-TRPV1–expressing HEK293 cells treated with dynasore, a reversible, noncompetitive dynamin inhibitor that can permeate the cell membrane. Dynasore-treated cells showed an increase in surface TRPV1 compared with vehicle-treated cells (Fig. 2E). Mutations of lysine 44 in the guanosine 5′-triphosphate–binding domain of dynamin (K44A or K44E) abolished endocytosis (*32*, *33*). Overexpression of wild-type dynamin reduced surface TRPV1 abundance, whereas overexpression of dynamin carrying a dominant negative mutation (K44A) reversed this effect (Fig. 2F). In summary, the internalization of TRPV1 depended on clathrin and dynamin.

AP2μ2 is essential for TRPV1 internalization

In the clathrin-dependent internalization pathway, the AP2 complex plays a crucial role by interacting with clathrin, phosphatidylinositol 4,5-bisphosphate (PIP_2, a minor phospholipid component of cell membranes), and the target protein. During this process, the μ2 subunit of the AP2 complex is responsible for binding to the cargo protein (*34*). We observed colocalization of TRPV1 and AP2μ2 in HEK293 cells (Fig. 3A). Bioinformatics analysis revealed several sequences in TRPV1 [YNEI (tyrosine-asparagine-glutamic acid-isoleucine) at positions 309 to 312, YGPV (tyrosine-glicine-proline-valine) at positions 374 to 377, and YAVM (tyrosine-alanine-valine-methionine) at positions 565 to 568] that could be recognized by AP2μ2 and therefore mediate the interaction between TRPV1 and AP2μ2 (*34*). We constructed plasmids encoding the fusion proteins glutathione *S*-transferase (GST)–AP2μ2 and His-tagged TRPV1 C- and N-terminal amino acid fragments (His-TRPV1-CT and His-TRPV1-NT) and used the purified proteins for in vitro pull-down assays. His-TRPV1-NT pulled down GST-AP2μ2, but His-TRPV1-CT did not, indicating a direct interaction of the N terminus of TRPV1 with AP2μ2 (Fig. 3B). We also performed a GST pull-down experiment in HEK293 cells expressing GST-TRPV1 and His-Myc-AP2μ2. The results showed that GST-TRPV1 pulled down His-Myc-AP2μ2 (Fig. 3C), indicating that TRPV1 and AP2μ2 interacted with each other in cells. In addition to the physical interaction between TRPV1 and AP2μ2, we also found that overexpression of AP2μ2 in HEK293 cells reduced the membrane surface abundance of TRPV1 compared with the vector control group (Fig. 3D). Knockdown of AP2μ2 using a siRNA previously shown to reduce the abundance of endogenous AP2μ2 (*24*) increased the membrane surface abundance of TRPV1 compared with the nonsilenced control group (Fig. 3E). The above results show that AP2μ2 was necessary for TRPV1 internalization.

TRPV1 internalization is negatively regulated by CDK5-mediated phosphorylation of AP2μ2

Previous results from our group demonstrated that CDK5 increases the transport of TRPV1 to the cell membrane through the phosphorylation of the kinesin motor protein KIF13B (*20*). To investigate whether CDK5 affects the internalization of TRPV1, we used the CDK5 inhibitor roscovitine to pretreat HEK293 cells before the

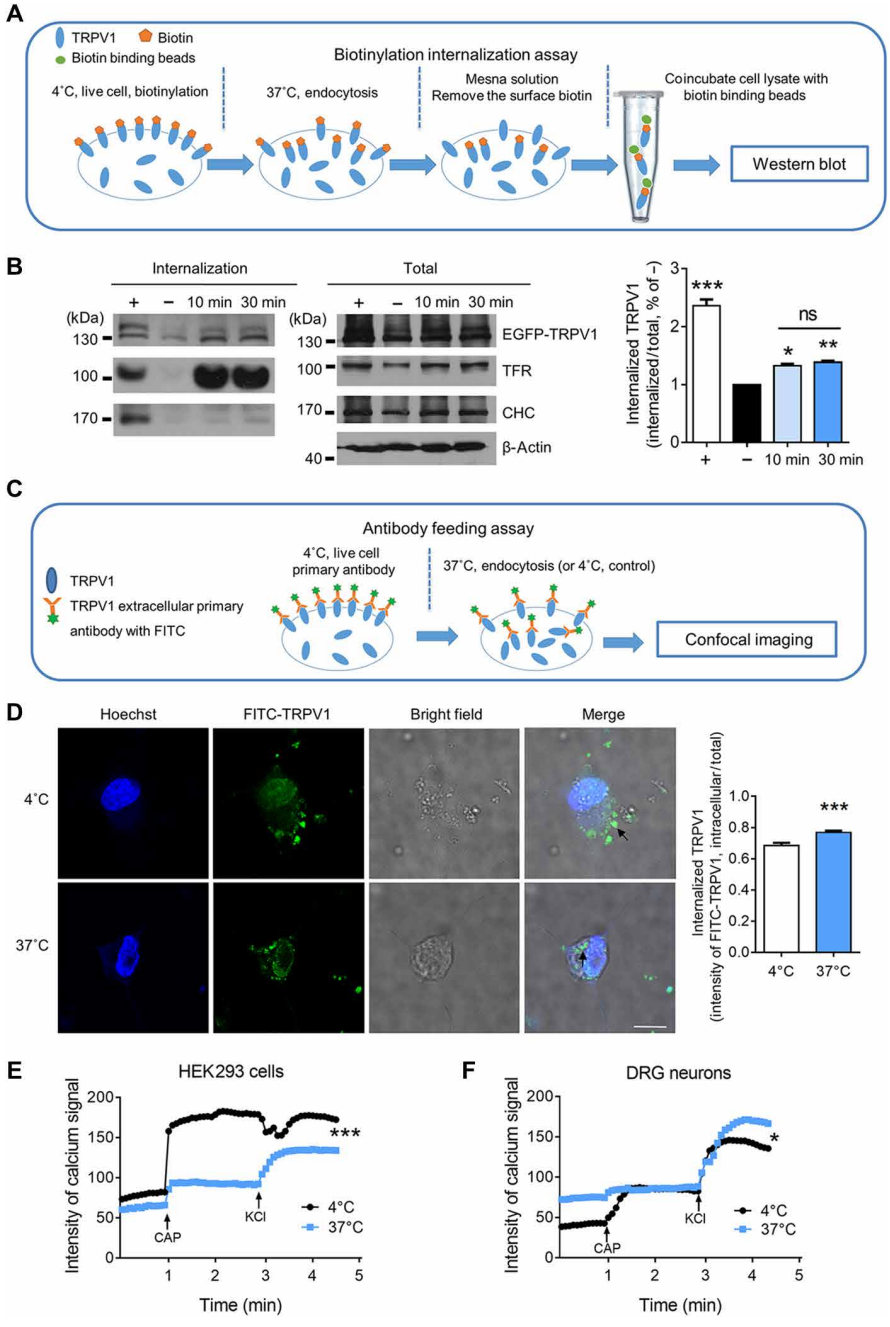

Fig. 1. Constitutive internalization of TRPV1. (**A**) Schematic diagram of the biotinylation internalization assay. (**B**) Representative Western blot for TRPV1, transferrin receptor (TFR), and clathrin heavy chain (CHC) in biotinylation internalization assays in HEK293 cells transfected with EGFP-TRPV1 plasmid. Internalized proteins were analyzed by treating the cells with mesna solution to remove the surface biotin. β-Actin is a loading control. The bar graph shows quantitation of the ratio of internalized TRPV1 normalized to the negative control (–) in which the biotinylated cells were incubated at 37°C for 0 min. As a positive control (+), there was no mesna solution treatment to remove surface biotinylation after internalization. Data represent means ± SEM of three independent experiments. $^{*}P < 0.05$, $^{**}P < 0.01$, $^{***}P < 0.001$ by one-way analysis of variance (ANOVA), followed by Tukey's multiple comparison test. ns, not significant. (**C**) Schematic diagram of the antibody feeding assay to measure internalization of endogenous TRPV1. (**D**) Representative images and quantification of the antibody feeding assay in primary DRG neurons. Scale bar, 10 μm. Data represent means ± SEM of 29 neurons (4°C group) and 41 neurons (37°C group) from three independent experiments. $^{***}P < 0.001$ by the two-tailed paired *t* test. (**E** and **F**) Representative traces showing the typical average change in Ca^{2+} influx in HEK293 cells (E) or primary DRG neurons (F) in each treatment group. Application of capsaicin (CAP) and KCl is indicated by arrows. Data represent means ± SEM of 50 cells for each group from three independent experiments; $^{*}P < 0.05$, $^{***}P < 0.001$ by two-way ANOVA.

biotinylation internalization assay. The results showed an enhancement of the internalization of TRPV1 in the roscovitine pretreatment group compared with the vehicle control group (Fig. 4A). Simultaneously, roscovitine pretreatment also enhanced the interaction between TRPV1 and AP2μ2 in the GST pull-down assay compared with the vehicle control group (Fig. 4B). The internalization of TRPV1 increased in HEK293 cells expressing short hairpin RNAs (shRNAs) directed against CDK5 (shCDK5) or the CDK5 activator p35 (shP35) (Fig. 4C), indicating that both the amount and the activity of CDK5 affected TRPV1 internalization.

By bioinformatics analysis, we found three potential CDK5 phosphorylation sites in AP2μ2: Ser^{45}, Ser^{186}, and Thr^{326}. To test whether CDK5 could phosphorylate AP2μ2, we performed in vitro ^{32}P radioisotope kinase activity tests with four purified GST-tagged fragments of AP2μ2 (amino acids 1 to 100, 101 to 207, 201 to 300, and 301 to 435). Cdk5 phosphorylated only the 1 to 100 amino acid peptide segment of AP2μ2 (Fig. 4D). To determine whether AP2μ2 and CDK5 interacted in cells, we performed pull-down experiments in HEK293 cells expressing His-tagged CDK5 (His-CDK5) and GST-AP2μ2. GST-AP2μ2 pulled down His-CDK5, indicating that CDK5 directly interacted with APμ2 (Fig. 4E). Ser^{45}, the candidate CDK5 phosphorylation site in the 1 to 100 amino acid peptide segment of AP2μ2, is conserved in many species. A mutant version of this peptide in which this residue was replaced with alanine (S45A) was not phosphorylated by Cdk5 in the ^{32}P radioisotope kinase activity test, confirming that this site was phosphorylated by Cdk5 (Fig. 4F). Furthermore, GST-AP2μ2 pulled down endogenous Cdk5 from mouse brain tissue extracts, but GST-$AP2\mu2^{S45A}$ did not (Fig. 4G). Last, we generated an antibody specific for AP2μ2 phosphorylated at Ser^{45} and used it to examine AP2μ2 phosphorylation when CDK5 was inhibited. When we pretreated HEK293 cells with roscovitine to inhibit CDK5 activity or transfected cells with shCDK5 plasmids to suppress CDK5 translation, the phosphorylation of AP2μ2 was decreased compared to control groups pretreated with vehicle or expressing the empty vector

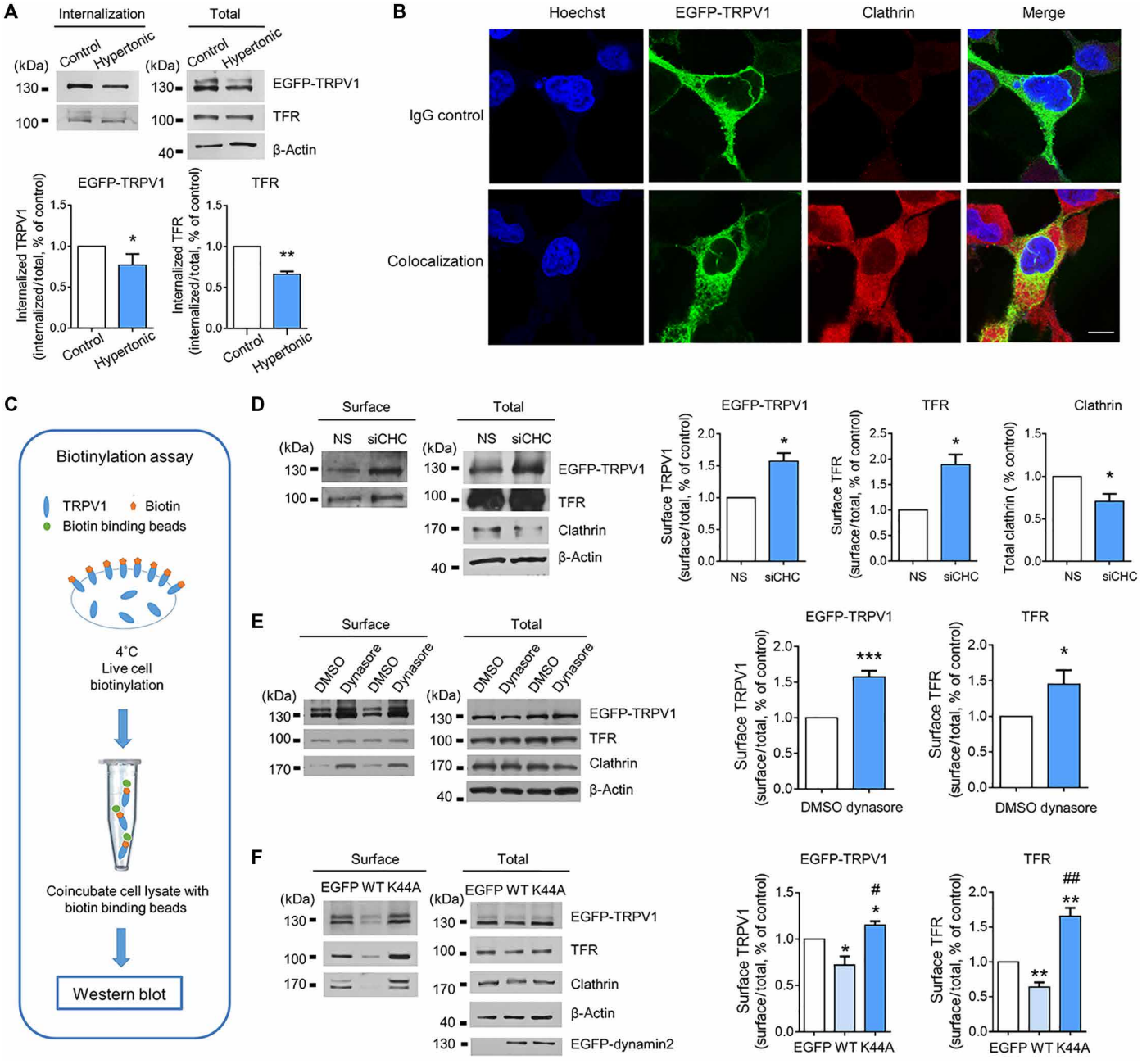

Fig. 2. TRPV1 internalization depends on clathrin and dynamin. (**A**) Representative Western blot for TRPV1 and TFR in biotinylation internalization assays in HEK293 cells expressing EGFP-TRPV1 and subjected to hypertonic treatment. The ratio of internalized TRPV1 or TFR normalized to the control group was quantified. Data represent means ± SEM of three independent experiments. *$P < 0.05$, **$P < 0.01$ by the one-tailed paired *t* test. (**B**) Representative images of HEK293 cells showing the distribution of EGFP-TRPV1 and clathrin. Cells stained with immunoglobulin G (IgG) are a negative control for clathrin staining. Scale bar, 10 μm. $n = 20$ cells from three independent experiments. (**C**) Schematic diagram of the biotinylation assay to quantify TRPV1 on the cell surface. (**D**) Representative Western blot for TRPV1, TFR, and clathrin in biotinylation assays in HEK293 cells coexpressing EGFP-TRPV1 and siRNA targeting CHC (siCHC). Surface TRPV1, surface TFR, and total CHC were quantified and normalized to the nonsilencing siRNA (NS) group. Data represent means ± SEM of three independent experiments. *$P < 0.05$ by the one-tailed paired *t* test. (**E**) Representative Western blot for TRPV1, TFR, and clathrin in biotinylation assays in HEK293 cells expressing EGFP-TRPV1 and treated with the dynamin inhibitor dynasore or vehicle (DMSO). Surface TRPV1 and TFR were quantified and normalized to the DMSO control group. Data represent means ± SEM of three independent experiments. *$P < 0.05$, ***$P < 0.001$ by the one-tailed paired *t* test. (**F**) Representative Western blot for TRPV1, TFR, clathrin, and EGFP in biotinylation assays in HEK293 cells coexpressing EGFP-TRPV1 plus EGFP-dynamin (WT), EGFP-DN-dynamin (K44A), or EGFP vector alone (EGFP). Surface TRPV1 and surface TFR were quantified and normalized to the EGFP vector control group. Data represent means ± SEM of three independent experiments. *$P < 0.05$, **$P < 0.01$, #$P < 0.05$, and ##$P < 0.01$ by the one-tailed paired *t* test.

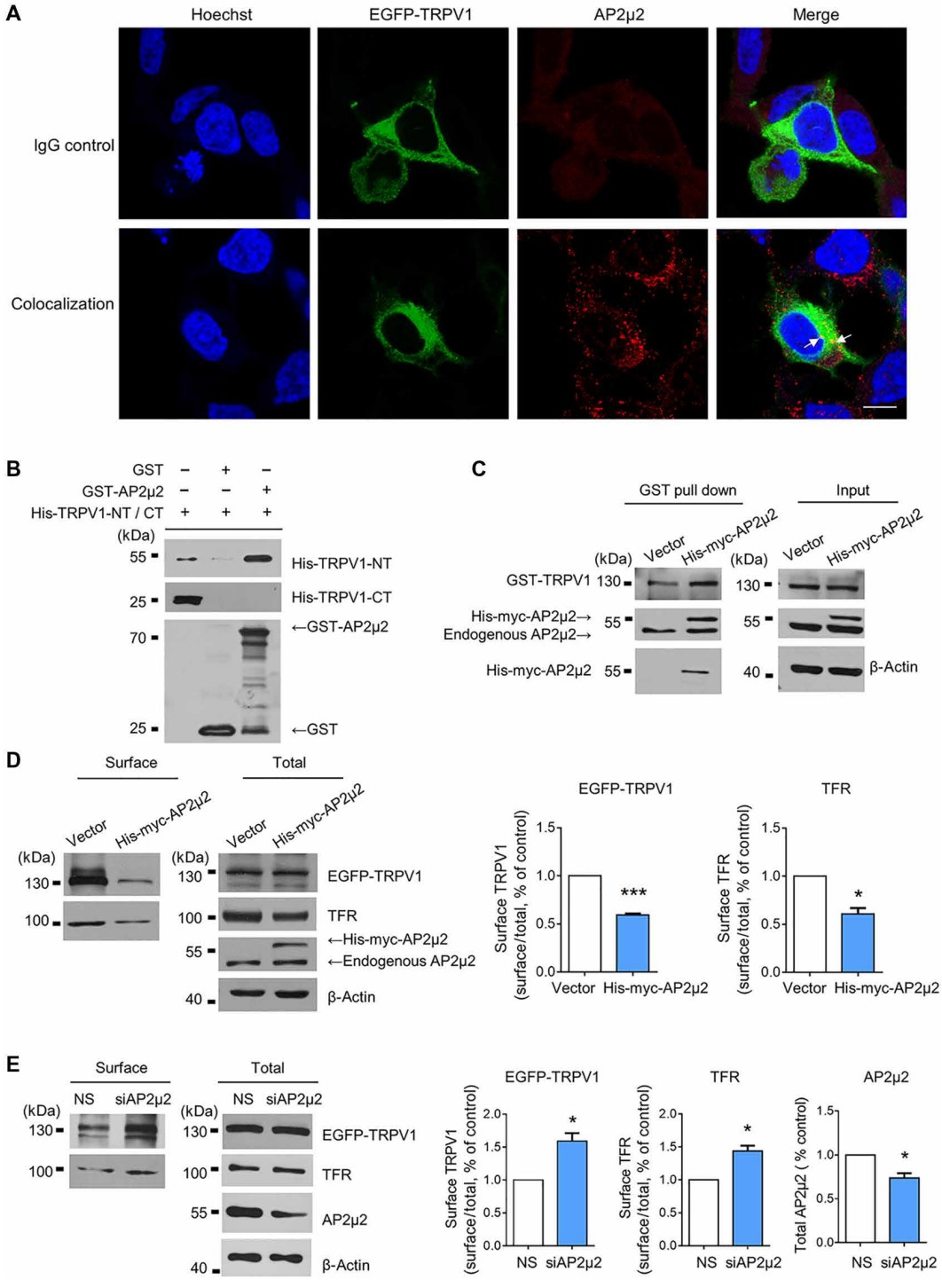

Fig. 3. TRPV1 internalization depends on AP2μ2. (**A**) Representative images showing the distribution of TRPV1 and AP2μ2 in HEK293 cells. Cells stained with IgG is a negative control for the AP2μ2 antibody. Scale bar, 10 μm. $n = 20$ cells from three independent experiments. (**B**) Western blot of in vitro pull-down assays using purified recombinant His-TRPV1-NT, His-TRPV1-CT, GST-AP2μ2, and GST alone. The immunoblots were probed with an antibody against the His tag. Blot is representative of three independent experiments. (**C**) Western blot of GST pull-down assays in HEK293 cells coexpressing GST-TRPV1 and either His-Myc-AP2μ2 or the His-Myc vector alone. The immunoblot was probed with antibodies against GST, AP2μ2, and the His tag. Blot is representative of three independent experiments. (**D** and **E**) Representative Western blot for biotinylation assay in HEK293 cells cotransfected with EGFP-TRPV1 and either His-Myc-AP2μ2 plasmids (D) or AP2μ2 siRNA (E). Surface TRPV1, surface TFR, and total AP2μ2 were quantified and normalized to the His-Myc vector alone or nonsilencing siRNA (NS) control group. Data represent means ± SEM of three independent experiments. $^*P < 0.05$, $^{***}P < 0.001$ by the one-tailed paired *t* test.

(Fig. 4, H and I). Thus, CDK5 bound to and phosphorylated AP2μ2 Ser^{45} to negatively regulate TRPV1 internalization.

Interfering with phosphorylation of AP2μ2 at Ser^{45} enhances TRPV1 internalization

To investigate the effect of CDK5-mediated AP2μ2 Ser^{45} phosphorylation on TRPV1 internalization, we generated a cell-penetrating peptide corresponding to a region of AP2μ2, including Ser^{45}. We fused residues 38 to 52 of AP2μ2 to the cell-permeable HIV TAT protein sequence RKKRRQRRR (TAT-S45). As a control, we also generated a peptide in which Ser45 was replaced with alanine (TAT-S45A) (Fig. 5A). Other researchers and our previous studies have confirmed that peptides representing specific phosphorylation sites can disrupt phosphorylation at the site in the endogenous substrate (*20*, *35*, *36*). TAT-S45 and the control peptide TAT-S45A were added to the radioisotope kinase activity assay with CDK5 and AP2μ2. The TAT-S45 peptide reduced the phosphorylation of AP2μ2 by CDK5 compared to the TAT-S45A peptide (Fig. 5B). We also tested the ability of these peptides to interfere with the internalization of TRPV1 in cells. HEK293 cells were pretreated with TAT-S45 or TAT-S45A before the biotinylation assay. In the TAT-S45–pretreated cells, the abundance of TRPV1 on the cell surface decreased (Fig. 5C), and the internalization of TRPV1 increased (Fig. 5D) compared with the TAT-S45A control groups. The interaction of TRPV1 with AP2μ2

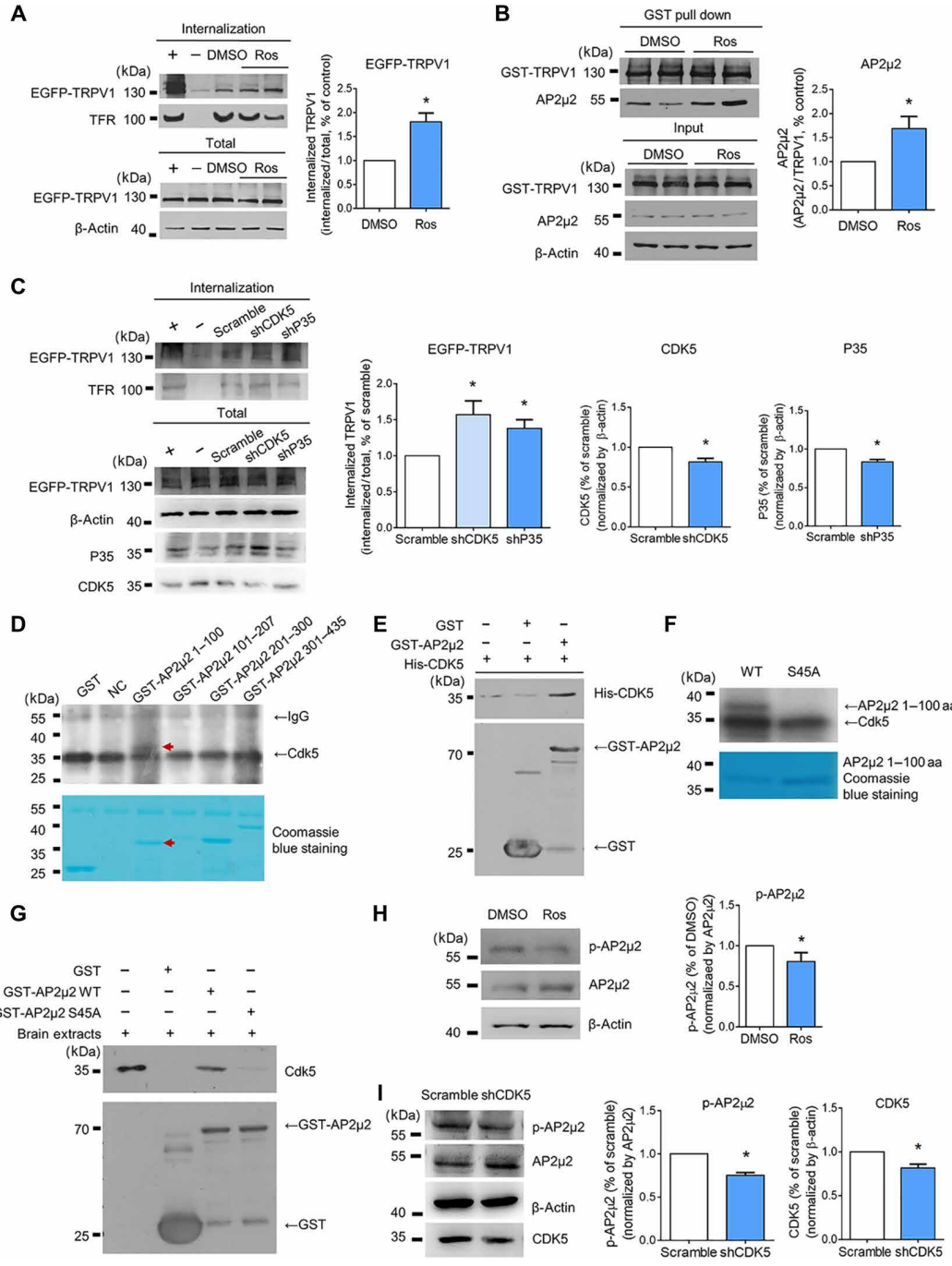

Fig. 4. CDK5 negatively regulates TRPV1 internalization by phosphorylating AP2μ2. (**A**) Representative Western blot for biotinylation internalization assay in HEK293 cells transfected with EGFP-TRPV1 and treated with roscovitine (Ros) or vehicle (DMSO). Internalized TRPV1 was quantified and normalized to the vehicle control group. (**B**) Representative Western blot for GST pull-down assay in HEK293 cells transfected with GST-TRPV1 plasmids and treated with roscovitine or vehicle. AP2μ2 was quantified and normalized to the vehicle control group. (**C**) Representative Western blot for biotinylation internalization assay in HEK293 cells cotransfected with EGFP-TRPV1 and shRNAs against CDK5 (shCDK5), P35 (shP35), or a scrambled control. Internalized TRPV1 was quantified and normalized to the scrambled control group. (**D**) Representative Western blot and autoradiogram for in vitro kinase assay using Cdk5 immunoprecipitated from mouse brain lysates incubated with the indicated GST-tagged fragments of AP2μ2 in the presence of radiolabeled adenosine 5′-triphosphate (ATP). (**E**) Representative Western blot for the His tag in GST pull-down assays using purified recombinant GST-AP2μ2 and His-CDK5. (**F**) Representative Western blot and autoradiogram for in vitro kinase assay using Cdk5 immunoprecipitated from mouse brain lysates and incubated with GST-AP2μ2 1 to 100 amino acids or mutant GST-AP2μ2 1 to 100 amino acids (S45A) in the presence of radiolabeled ATP. (**G**) Representative Western blot for Cdk5 in GST pull-down assays using GST-AP2μ2 1 to 100 amino acids or mutant GST-μ2 1 to 100 amino acids (S45A) against mouse brain lysates. (**H**) Representative Western blot and quantification of AP2μ2 phosphorylated at Ser^{45} (p-AP2μ2) in HEK293 cells treated with roscovitine or vehicle. (**I**) Representative Western blot and quantification of AP2μ2 phosphorylated at Ser^{45} in HEK293 cells cotransfected with EGFP-TRPV1 and shRNAs against CDK5. For all panels, $n = 3$ independent experiments. Data represent means ± SEM. *$P < 0.05$ by the one-tailed paired t test.

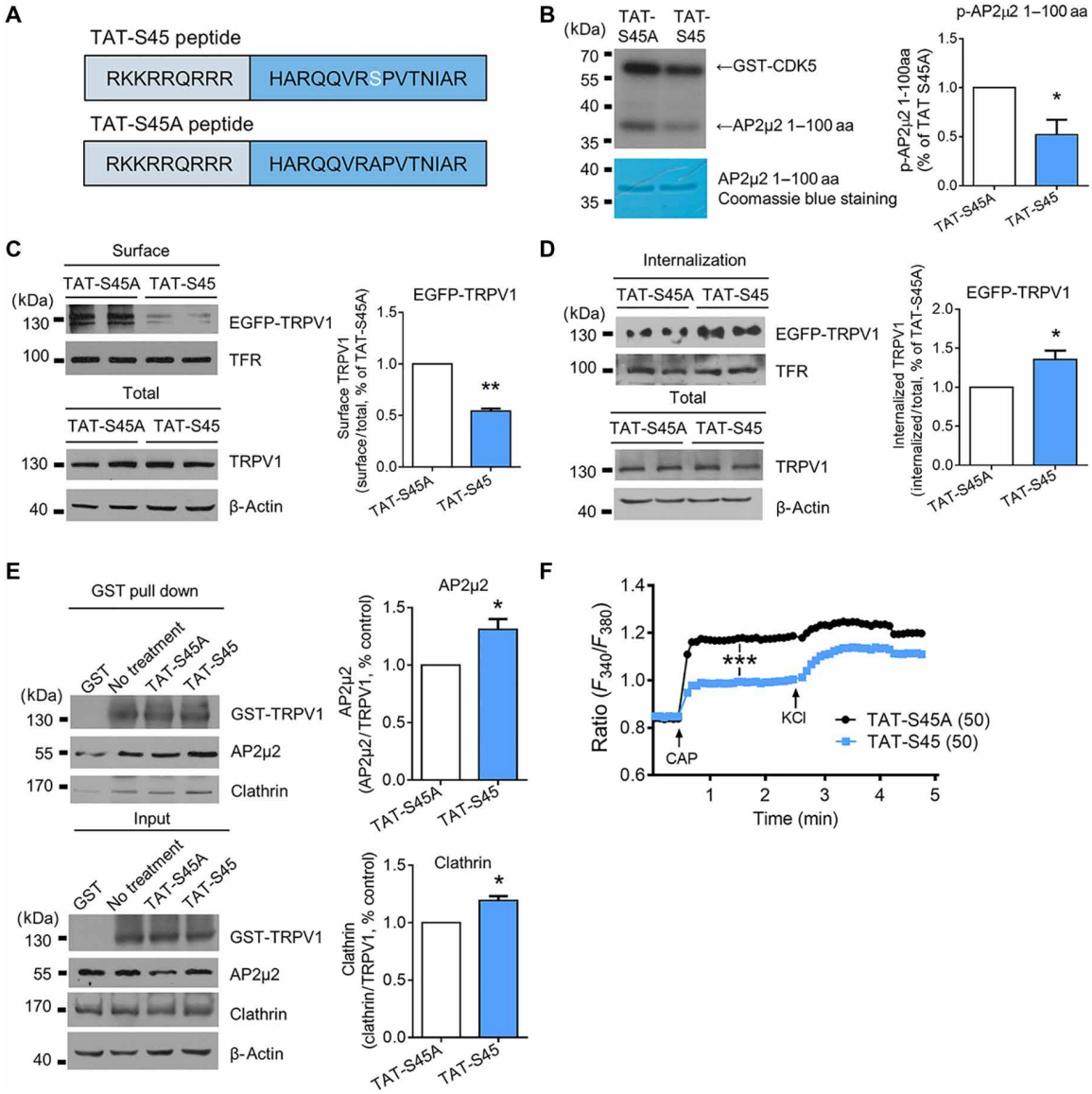

Fig. 5. The TAT-S45 fusion peptide enhances TRPV1 internalization. (**A**) Schematic diagram of the TAT-S45 peptide and TAT-S45A control peptide. (**B**) Representative Western blot and autoradiogram for in vitro kinase assay. P35 was immunoprecipitated from mouse brain lysates and incubated with GST-CDK5 and GST-μ2 1 to 100 amino acids in the presence of radiolabeled ATP plus the TAT-S45 or TAT-S45A peptide. P-AP2μ2 1 to 100 amino acids was quantified and normalized to the TAT-S45A control group. Data with means ± SEM of three independent experiments; $^{*}P < 0.05$ by the one-tailed paired *t* test. (**C** and **D**) Representative Western blots for biotinylation assays (C) or biotinylation internalization assays (D) in HEK293 cells transfected with EGFP-TRPV1 plasmids after TAT-S45 or TAT-S45A peptide treatment. Surface TRPV1 (C) and internalized TRPV1 (D) were quantified and normalized to the TAT-S45A control group. Data represent means ± SEM of three independent experiments; $^{*}P < 0.05$, $^{**}P < 0.01$ by the one-tailed paired *t* test. (**E**) Representative Western blot showing GST-TRPV1 and AP2μ2 in GST pull-down assays from lysates of HEK293 cells expressing GST-TRPV1 and treated with TAT-S45 or TAT-S45A peptide. AP2μ2 and clathrin were quantified and normalized to the TAT-S45A control group. Data with means ± SEM of three independent experiments; $^{*}P < 0.05$ by the one-tailed paired *t* test. (**F**) Representative traces showing the typical average change in Ca^{2+} influx of HEK293 cells in each group. Application of capsaicin (CAP) and KCl is indicated by arrows. Data with means ± SEM of 50 cells for each group from three independent experiments; $^{***}P < 0.001$ by two-way ANOVA.

and clathrin also increased in cells pretreated with TAT-S45 (Fig. 5E). To observe the functional consequences of the AP2μ2-competitive peptide on TRPV1 activity, we performed Ca^{2+} imaging with Fura-2 in HEK293 cells pretreated with TAT-S45 or TAT-S45A. The results showed a reduction in the activation of surface TRPV1 by capsaicin in the TAT-S45–pretreated group (Fig. 5F). In conclusion, inhibiting phosphorylation of AP2μ2 at Ser^{45} by CDK5 increased TRPV1 internalization and reduced the amount and activity of surface TRPV1.

Phosphorylation of AP2μ2 at Ser^{45} contributes to the development of inflammatory thermal hyperalgesia in rats

Because both Cdk5 and TRPV1 have important roles in inflammatory thermal hyperalgesia, we applied the complete Freund's adjuvant (CFA)–induced inflammatory pain rat model to study the biological effect of TRPV1 internalization and its negative regulation by Cdk5. DRGs were harvested at various times after injection of CFA into a hind paw to detect the Ser^{45} phosphorylation of AP2μ2. At 6 hours

after CFA injection, there was an enhancement of AP2μ2 Ser^{45} phosphorylation (Fig. 6A). Intrathecal administration of the Cdk5 inhibitor roscovitine reduced AP2μ2 Ser^{45} phosphorylation with or without CFA injection (Fig. 6B). In addition to cell surface trafficking, axonal transport is also important for TRPV1-induced pain, and CFA increases the abundance of TRPV1 at peripheral nerve terminals through the activation of nerve growth factor (NGF) and p38 (*37*). DRG tissues were isolated from rats intrathecally injected with the TAT-S45 or TAT-S45A peptide and separated into three segments (central nerve terminals, DRG soma, and peripheral nerve terminals). Treatment with the TAT-S45 peptide increased the abundance of TRPV1 in the DRG somas and central nerve terminals (Fig. 6C).

To test the analgesic effect of the TAT-S45 peptide, we conducted behavioral experiments, assaying pain responses to TRPV1 stimulation. Rats were intrathecally injected with the TAT-S45 or TAT-S45A peptide before capsaicin injection into a hind paw, and spontaneous pain behavior was assayed by counting the total time the paw was lifted in the first 5 min after injection. TAT-S45 shortened the lifting duration compared to TAT-S45A (Fig. 6D). Intrathecal injection of the TAT-S45 peptide had no effect on the heat-evoked paw-withdrawal latency (PWL) compared to rats injected with TAT-S45A (Fig. 6E). Compared to intrathecal injection of the TAT-S45A control peptide, intrathecal injection of TAT-S45 before injection of CFA into a hind paw enhanced heat-evoked PWL at 2 and 6 hours after CFA injection, and the pain inhibition effect disappeared 1 day after the induction of inflammation (Fig. 6F). Whereas injection of 10 μg of TAT-S45 reduced inflammatory thermal hyperalgesia relative to TAT-S45A, injection of 3 or 30 μg did not, indicating that there was an optimal concentration of the peptide for pain relief (Fig. 6, G and H). These results suggest that disruption of AP2μ2 Ser^{45} phosphorylation with TAT-S45 peptide attenuated the spontaneous pain and inflammatory thermal hyperalgesia in rats.

DISCUSSION

In this study, we have provided evidence that TRPV1 is internalized through a clathrin-dependent pathway that is mediated by the binding of the N terminus of TRPV1 to AP2μ2 (Fig. 7A). CDK5 phosphorylated AP2μ2 at Ser^{45} to inhibit the interaction between TRPV1 and AP2μ2, leading to decreased TRPV1 internalization (Fig. 7B). The phosphorylation of AP2μ2 Ser^{45} increased in DRGs in the CFA-induced inflammatory hyperalgesia rat model, and the intrathecal delivery of a peptide that competes with endogenous AP2μ2 for Cdk5 (TAT-S45) effectively inhibited the negative regulation of TRPV1 internalization by Cdk5 and attenuated inflammatory thermal hyperalgesia in rats (Fig. 7C).

We observed constitutive internalization of surface TRPV1 both in HEK293 cells and in DRG neurons, and preventing constitutive internalization under the basal conditions increased TRPV1 activity as assessed by capsaicin-induced Ca^{2+} imaging (Fig. 1). It has been reported that TRPV1 is internalized and degraded after activation by capsaicin (*16*), yet few studies have focused on the constitutive internalization of TRPV1 that contributes to maintenance of the balance of recycling and surface stabilization of TRPV1. Regarding the mechanism of TRPV1 internalization, our results showed that TRPV1 interacted with AP2μ2 (Fig. 3, B and C). The AP2μ2 subunit is responsible for binding to cargo in clathrin-dependent endocytosis. AP2μ2 substrates usually contain the conservative binding motif YXXφ, in which φ represents hydrophobic amino acids and X represents any amino acid (*32*). Through bioinformatics analysis, we found possible AP2μ2 binding motifs in the N terminus of rat TRPV1 located at positions 309 to 312 (YNEI) and 374 to 377 (YGPV). Overexpression of AP2μ2 or dynamin decreased the distribution of surface TRPV1, whereas reducing or inhibiting endogenous clathrin, dynamin, or AP2μ2 increased the amount of surface TRPV1 (Figs. 2 and 3), indicating that TRPV1 constitutive internalization occurred in a clathrin-, dynamin-, and AP2μ2-dependent manner.

TRPV1 membrane trafficking affects many physiological processes. Exposure of skin cells to ultraviolet radiation causes Src-mediated TRPV1 trafficking to the cell membrane and, after Ca^{2+} influx, activates the interleukin-6 (IL-6)–IL-8–tumor necrosis factor–α–related signaling pathway, leading to skin inflammation or photoaging (*38*). TRPV1-dependent excitation of liver-related paraventricular nucleus neurons diminishes in type 1 diabetic mice and is restored by insulin in a manner that depends on phosphatidylinositol 3-kinase (PI3K) and protein kinase C (PKC) and stimulates TRPV1 trafficking to the membrane (*39*). Loss of insulin signaling may contribute to TRPV1 internalization in synaptic terminals (*39*). The lung epithelium is a frontline barrier to inhaled xenobiotics and pathogens. This important cell layer is often subjected to damage, possibly causing airway inflammation, pulmonary edema, various systemic responses, and respiratory dysfunction. TRPV1 antagonists can increase TRPV1 on the cell surface and exacerbate TRPV1-mediated toxicities in human lung epithelial cells (*40*). The mechanism of constitutive TRPV1 internalization we describe likely contributes to the steady-state abundance of surface TRPV1, thereby influencing diverse physiological activities of TRPV1.

In *Mycbp2* knockout mice, formalin-induced thermal hyperalgesia increases, suggesting that inhibition of TRPV1 internalization might be one of the mechanisms of inflammatory thermal hyperalgesia (*27*). Our previous studies have shown that, in a CFA-induced rat inflammatory pain model, Cdk5 activity increases in nociceptive neurons, promoting inflammatory sensitization by increasing TRPV1 transport to the surface of the cell membrane and to peripheral nerve terminals (*19*, *20*, *41*). Although it is a member of the cyclin-dependent kinase family, CDK5 does not seem to play a role in the cell cycle, but it has been implicated in various processes in the nervous system, including neuronal migration and differentiation, membrane transport, synaptogenesis, axon guidance, neurodegenerative disease, and pain signaling (*42*). Therefore, we investigated whether CDK5 affected TRPV1 internalization and its role in inflammatory hyperalgesia. Our results showed that pretreatment with roscovitine or expression of shCDK5 increased TRPV1 internalization (Fig. 4, A and C), indicating that the activity of CDK5 had a negative regulatory effect on TRPV1 internalization. The consensus phosphorylation site of CDK5 is (S/T)PX(K/H/R) (*43*). We identified three possible CDK5 phosphorylation sites in AP2μ2 (Ser^{45}, Thr^{156}, and Thr^{326}) and showed that CDK5 phosphorylated AP2μ2 at Ser^{45} (Fig. 4). Pretreatment with the TAT-S45 peptide weakened Ser^{45} phosphorylation by CDK5, increased the interaction between TRPV1 with AP2μ2 and clathrin, promoted TRPV1 internalization, and reduced the surface abundance of TRPV1, leading to a reduction in responsiveness to capsaicin (Fig. 5). In addition to CDK5, the NGF-PI3K pathway is also implicated in TRPV1 trafficking and function (*37*, *44*, *45*), and protein kinase A (PKA), PKC, and CaMKII, all of which can phosphorylate TRPV1, are also potential signal pathways regulating TRPV1 internalization (*10*, *46*, *47*).

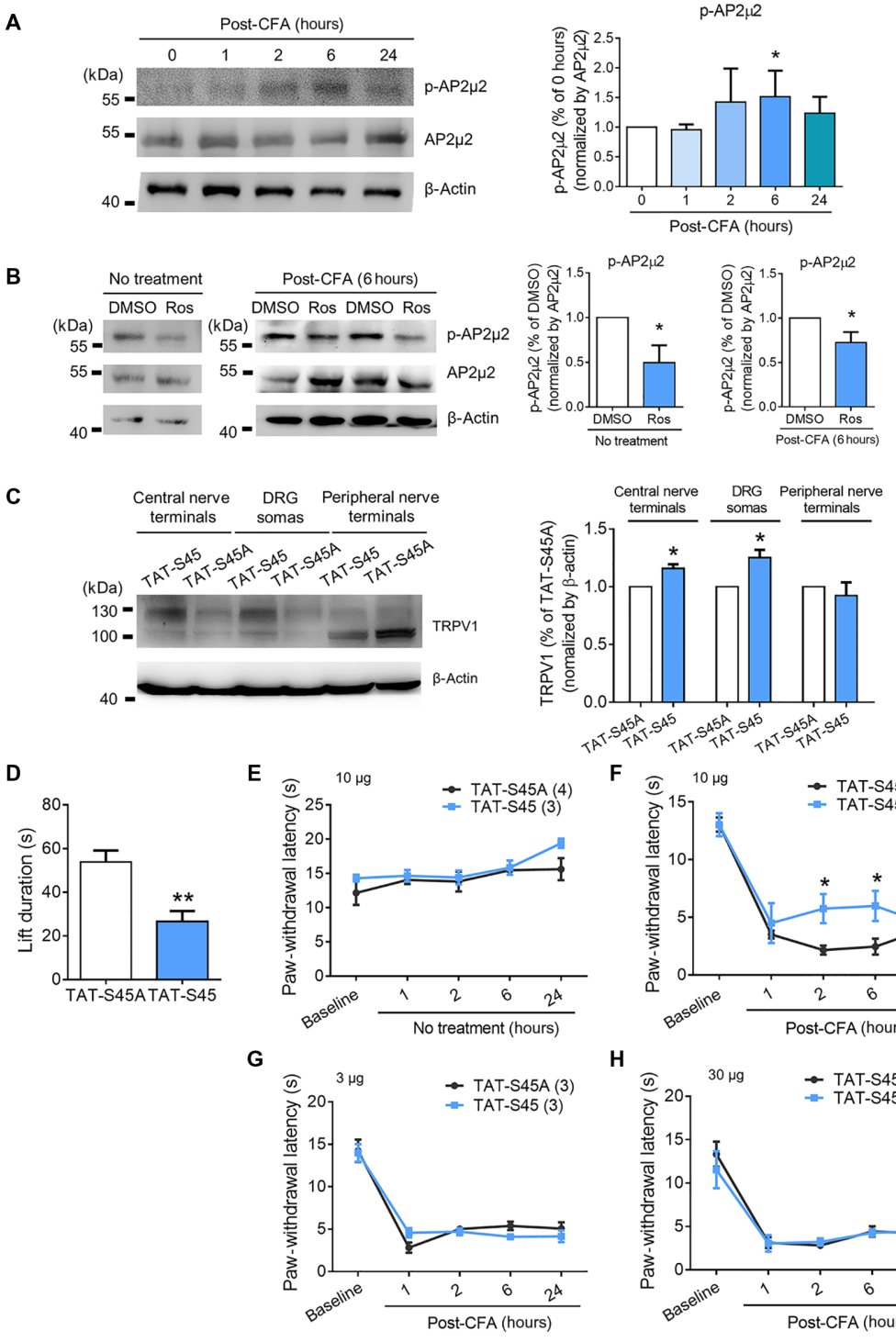

Fig. 6. Phosphorylation of AP2μ2 at Ser^{45} contributes to the development of inflammatory thermal hyperalgesia in rats. (**A** and **B**) Representative Western blot and quantification of Ap2μ2 phosphorylated at Ser^{45} (p-AP2μ2) in rat DRG tissues at the indicated times after injection with 25% CFA (A) or 6 hours after intrathecal injection with roscovitine or DMSO, followed by injection with 25% CFA (B). For quantitative analysis, p-AP2μ2 abundance was normalized to the 0-hour (A) or DMSO control (B) group. Data represent means ± SEM of three independent experiments. *$P < 0.05$ by the one-tailed paired *t* test. (**C**) Representative Western blot for TRPV1 in rat DRG tissues after intrathecal injection of TAT-S45A and TAT-S45 peptides. The bar graph shows the abundance of TRPV1 normalized to that in the TAT-S45A group. Data represent means ± SEM of three independent experiments. *$P < 0.05$ by the two-tailed paired *t* test. (**D**) Paw lifting time in the first 5 min after capsaicin injection into rats intrathecally injected with the TAT-S45A or TAT-S45 peptide. Data were analyzed by the two-tailed unpaired *t* test; **$P < 0.01$; $n = 8$ rats for each group. (**E** to **H**) Representative time course of the PWL of the ipsilateral hind paw as measured by radiant heat stimuli before and after intrathecal injection of 10 μg (E and F), 3 μg (G), or 30 μg (H) of TAT-S45 or TAT-S45A peptides, followed by no treatment (E) or injection of 25% CFA (F to H). Data represent means ± SEM of six to eight rats; *$P < 0.05$ by the two-way ANOVA followed by Bonferroni's post hoc tests.

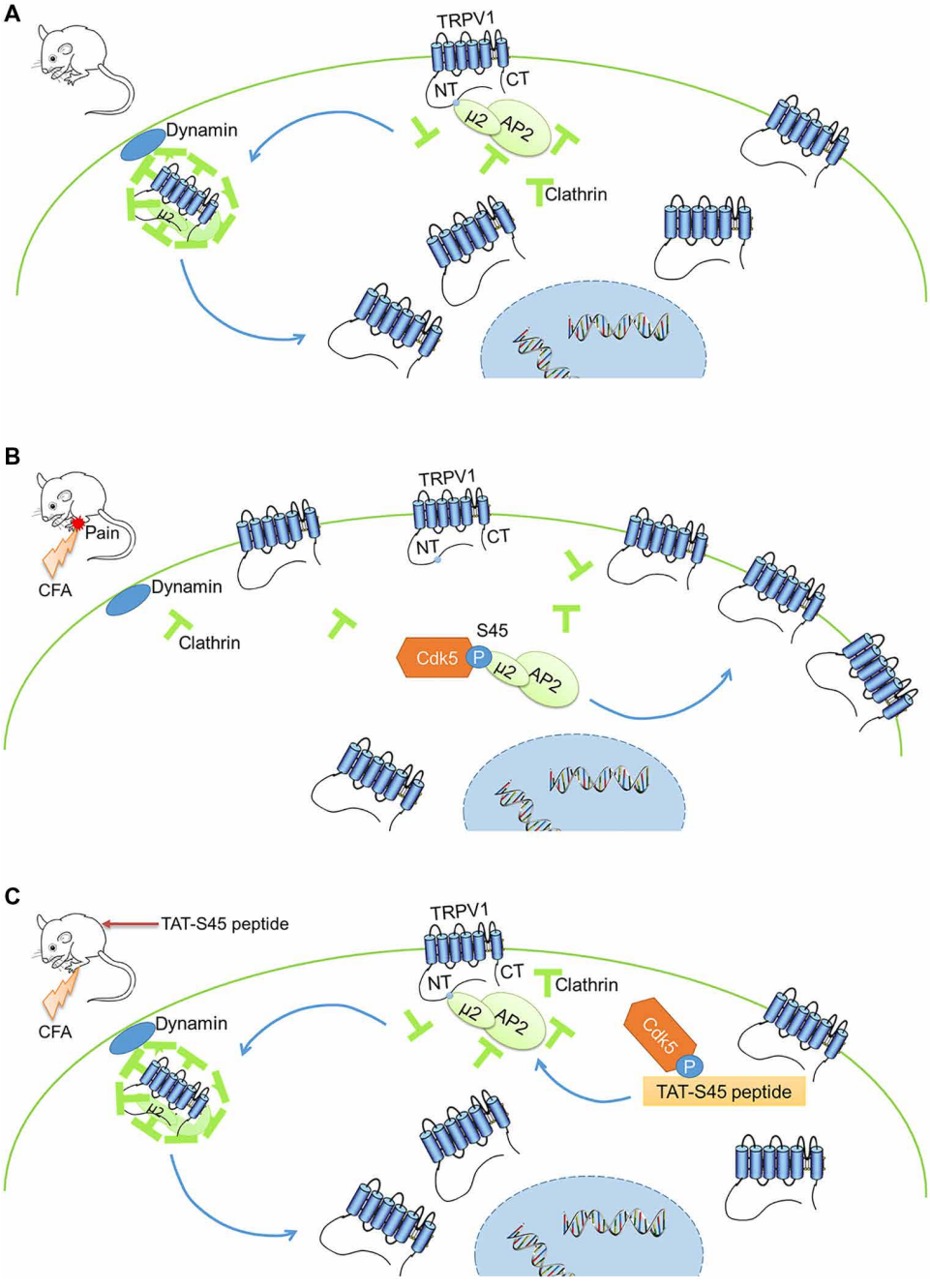

Fig. 7. Schematic model representing the TRPV1 internalization process and its regulation by CDK5. (**A**) Under basal conditions, AP2μ2 binds to the N terminus (NT) of TRPV1 and stimulates TRPV1 internalization through a clathrin- and dynamin-dependent pathway. (**B**) Cdk5 activity is increased in the context of peripheral inflammation, leading to the Cdk5-mediated phosphorylation of AP2μ2 at Ser^{45}, which negatively regulates TRPV1 internalization. (**C**) The TAT-S45 peptide competes with endogenous AP2μ2 for phosphorylation by Cdk5, thus antagonizing the Cdk5-dependent inhibition of TRPV1 internalization and reducing inflammatory hyperalgesia.

The mechanism of TRPV1 sensitization has received great attention for the development of effective analgesic methods. However, existing TRPV1 agonists and antagonists have not been satisfactory in clinical applications because of their low efficiency and tendency to cause burning pain, hyperthermia, or a reduced normal nociceptive response to heat (*48*). Inhibition of CDK5 activity is not a viable option for reducing TRPV1 surface abundance because it is likely to cause side effects related to inhibiting the other extensive physiological functions of CDK5. In the CFA-induced rat inflammatory pain model, the use of the peptide TAT-T506, which corresponds to the Cdk5 phosphorylation site in KIF13B, specifically interferes with the Cdk5-mediated phosphorylation of endogenous KIF13B, reduces the trafficking of TRPV1 to the cell membrane, and alleviates thermal hyperalgesia (*20*). Intrathecal injection of the peptide TAT-T406, which corresponds to the Cdk5 phosphorylation site in TRPV1, specifically interferes with the Cdk5-mediated phosphorylation of endogenous TRPV1, reduces the surface distribution of TRPV1, and alleviates thermal hyperalgesia (*19*). The amount of AP2μ2 Ser^{45} phosphorylation by Cdk5 increased in the CFA-induced inflammatory pain model, and intrathecal delivery of roscovitine weakened AP2μ2 Ser^{45} phosphorylation in vivo (Fig. 6, A and B). Intrathecal delivery of the peptide TAT-S45 alleviated both spontaneous pain and thermal hyperalgesia in the CFA-induced inflammatory pain model in rats (Fig. 6, D and F). Although TAT-S45 did not affect the internalization of TFR (Fig. 5, C and D), which confirmed the specificity of this peptide, it could not exclude the possibility that the CDK5-mediated phosphorylation of AP2μ2 may affect the internalization of other surface proteins that undergo clathrin-dependent internalization, and we could not rule out the possibility that TAT-S45 interferes with the CDK5-mediated phosphorylation of other targets besides AP2μ2.

Current research shows that 8 to 22% of the world's population suffers from chronic pain each year, and up to 50% of patients with chronic pain have a mental health comorbidity such as anxiety and depression, affecting daily life quality and causing an economic burden to families and society (*49*–*53*). More than 40% of patients still suffer from inadequate control of pain (*54*). Because of the various side effects or the poorly curative effects of marketed drugs, effective and specific treatment methods for pain thus far remain elusive (*55*, *56*). It is an urgent and arduous task to develop new analgesic drugs that have high efficiency, minimal side effects, and convenient methods of delivery. Selectively targeting mechanisms that control TRPV1 internalization may provide new strategies for the clinical management of inflammatory pain.

To summarize, our study has revealed that constitutive TRPV1 internalization occurred through a clathrin-, dynamin-, and AP2μ2-dependent mechanism. In this process, there was a direct interaction between TRPV1 and AP2μ2. CDK5 phosphorylated AP2μ2 at Ser^{45}, which reduced the binding between TRPV1 and AP2μ2, thus negatively regulating TRPV1 internalization. Specific interference with the CDK5-mediated phosphorylation of AP2μ2 Ser^{45} increased TRPV1 internalization and alleviated the spontaneous pain response to capsaicin and CFA-induced inflammatory thermal hyperalgesia in rats. Our study provides a detailed mechanism of TRPV1 internalization and a new potential target for clinical analgesic treatment.

MATERIALS AND METHODS

Cell culture and transfection

HEK293 cells were recovered from liquid nitrogen and cultured in 3.5-cm dishes with Dulbecco's modified Eagle's medium (DMEM) supplemented with 10% fetal bovine serum (FBS) (HyClone) at 5% CO_2 and 37°C in a water-saturated atmosphere. Half of the culture medium was exchanged every 2 days. When the cell density reached about 80 to 100%, the cells were digested with 0.25% trypsin and divided equally into three 3.5-cm dishes. Transfection was performed 24 hours after cell propagation when the cell density reached 60 to 70% using Lipofectamine 2000 (Invitrogen). Cells were harvested for experiments 48 hours later. siRNA duplexes against different regions of the CHC and AP2μ2 sequence were designed and transfected as previously reported (*24*) and synthesized by GL Biochem (CHC siRNA sequence, 5′-uaauccgauucgaagaccaau-3′ and 5′-aauggaucucucugaauacgg-3′; AP2μ2 siRNA sequence, 5′-gaucaagcgcauggcaggcau-3′ and 5′-caguggaugccuuucgcguca-3′). The nonspecific duplex III (Dharmacon) was used as a control.

As described previously (*19*), DRGs aseptically removed from neonatal rats (10 to 15 days) were digested with collagenase D (1.5 mg/ml) (Sigma-Aldrich) for 45 min and 0.125% trypsin (Sigma-Aldrich) for 8 min at 37°C, followed by trituration with a flame-polished Pasteur pipette. Dissociated cells were collected and resuspended in plating medium (DMEM containing 10% FBS), and 2×10^5 DRG neurons were plated onto a 3.5-cm dish coated with poly-D-lysine (Sigma-Aldrich). After 3 hours, the medium was replaced with Neurobasal medium supplemented with 2% B27 and 2 mM GlutaMAX-I (Invitrogen). A total of 5 μM cytarabine (Sigma-Aldrich) was added to the culture 18 to 24 hours after plating and maintained until the end of the experiments. Cultured DRG neurons were treated with the TAT fusion peptides on day 3.

Plasmids, antibodies, and drugs

AP2μ2 or the truncations of AP2μ2 (amino acids 1 to 100, 101 to 207, 201 to 300, and 301 to 435) proteins tagged with GST were expressed from pGEX-5X-1. The N or C terminus of TRPV1 tagged with His6 was expressed from pET-28a (+). The shCDK5 and shP35 were cloned into pSUPER vector. Myc-His-AP2μ2 proteins were expressed from pcDNA 3.1. The plasmids EGFP-TRPV1 and GST-TRPV1 were constructed as described previously (*20*, *57*). Mutations (S45A) within the AP2μ2 were created with the QuikChange Site-Directed Mutagenesis Kit (Stratagene, CA). The plasmids EGFP-dynamin and EGFP-DN-dynamin (K44A) were obtained from the Addgene website. All plasmids were verified by DNA sequencing.

The antibodies recognizing TRPV1, GFP, CDK5, p35, and TFR were purchased from Santa Cruz Biotechnology (USA). The antibodies specific for clathrin and AP50 were purchased from BD Medical Technology (USA). The rabbit antibody with FITC tagged against extracellular TRPV1 domain was purchased from Alomone Labs (Israel). The antibody specific for AP2μ2 phosphorylated at Ser^{45} was generated by MBL Beijing Biotech Corporation. The antibodies specific for GST, His, and β-actin and all the secondary antibodies were purchased from Zhongshan Golden Bridge Biotechnology. All the fluorescent secondary antibodies were purchased from Invitrogen. Roscovitine, CFA, and incomplete Freund's adjuvant (IFA) were from Sigma-Aldrich. The TAT fusion peptides were synthesized by GL Biochem.

Western blot analysis

For protein separation, 10% polyacrylamide gels were run at 80 V for about 90 min and then 120 V until the loading buffer reached the bottom of the gel. Proteins were transferred to a nitrocellulose membrane (Pall Gelman Laboratory) using a wet blot transfer system (Bio-Rad Laboratories) for 2 hours at 150 mA. Membranes were blocked for 1 hour with 5% nonfat milk in TBS-T (tris-buffered saline with 0.05% Tween 20). Primary antibodies were incubated overnight at 4°C. After washing three times with TBS-T, the secondary antibody (1:2000, Sigma-Aldrich) was incubated overnight at 4°C. The signals were detected using ECL solution (Santa Cruz Biotechnology).

Cell surface biotinylation and internalization assays

Cells were pretreated for 1 hour in a hypertonic buffer (hypertonic, 0.45 M sucrose in the medium) or 30 min in dynasore (100 μM in the medium) before harvesting. EGFP-TRPV1 proteins present at the surface of HEK293 cells were biotinylated using EZ-Link NHS-LC-Biotin (for the biotinylation assay) or EZ-Link Sulfo-NHS-SS-Biotin (for the biotinylation internalization assay) (0.5 mg/ml, Pierce) in DPBS [8 g of NaCl, 2.9 g of $Na_2HPO_4 \cdot 2H_2O$, 0.2 g of KCl, 0.2 g of KH_2PO_4, 0.1 g of $MgCl_2 \cdot 6H_2O$, and 0.1 g of $CaCl_2$ (pH 7.4 to 7.6)] at 4°C for 30 min. Unreacted biotin was quenched using DPBS supplemented with 100 mM glycine (pH 7.4).

To assess surface biotinylation, cells were lysed using lysis buffer (1% Triton X-100 and 0.1% SDS in 1× TBS), and the supernatants from the cell lysates were incubated with UltraLink Plus immobilized streptavidin beads (Pierce) overnight at 4°C. After washing five times with lysis buffer, bound proteins were eluted by boiling for 5 min and analyzed by Western blot.

To assess internalization, cells were incubated at 37°C for the indicated times in culture medium. Biotin that remained at the cell surface was removed by incubation with fresh 100 mM mesna buffer [2-mercaptoethanesulfonic acid sodium salt (mesna) in 100 mM NaCl, 1 mM EDTA, and 50 mM tris-HCl (pH 8.6)] supplemented with 0.2% (w/v) bovine serum albumin three times (20 min each time) at 4°C. Last, the cells were washed with DPBS and then lysed in lysis buffer at 4°C. The biotinylated proteins in the supernatant were precipitated overnight from the Neutravidin-coupled beads (Pierce) and analyzed by Western blot.

Antibody feeding assay

After three washes with PBS (pH 7.4), primary cultured DRG neurons were incubated with an FITC-labeled antibody specific for the TRPV1 extracellular segment for 1 hour at 4°C (Alomone Labs). After three washes with PBS, the cells were transferred to 37°C for 30 min to allow membrane receptor internalization. Then, the cells were immediately

fixed with 4% paraformaldehyde (PFA) for 15 min at 4°C. After three washes with PBS, the cells were covered with 90% glycerol. Images were obtained using an inverted Leica true confocal scanner (TCS) SP8 microscope with an apochromatic (APO) 63× objective (oil, NA 1.4, zoom 7×). The fluorescence intensity was analyzed by Leica LAS X software.

Immunofluorescence

For analyses of the colocalization, HEK293 cells transfected with EGFP-TRPV1 were fixed with 4% PFA for 15 min at 4°C and blocked for 1 hour in 1% FBS and 0.1% Triton X-100. Primary antibodies were incubated at 4°C overnight. Alexa 594–conjugated secondary antibodies and Hoechst 33342 were used for 1 hour at room temperature. The stained sections were examined with an inverted Leica TCS SP8 microscope with an APO 63× objective (oil, NA 1.4, zoom 7×).

In vitro kinase assay

The in vitro kinase assay was conducted as described previously (*20*, *41*). Briefly, mouse brain extracts in kinase lysis buffer [50 mM tris (pH 7.4), 150 mM NaCl, 1.5 mM $MgCl_2$, 10% glycerol, 1% Triton X-100, 5 mM EGTA, leupeptin (0.51 g/ml), 1 mM phenylmethylsulfonyl fluoride, 1 mM Na_3VO_4, 10 mM NaF, and proteinase inhibitor cocktail] were immunoprecipitated with an anti-CDK5 antibody (1:100) at 4°C for 3 hours. The immunoprecipitates were washed four times with TBS containing 0.1% Triton X-100 and twice with kinase buffer [20 mM tris (pH 7.5), 20 mM $MgCl_2$, 1 mM EDTA, 1 mM EGTA, and 0.1 mM dithiothreitol], followed by resuspension and incubation in 25 μl of kinase buffer supplemented with [γ-^{32}P] ATP (10 μCi/50 μl), 0.1 mM dithiothreitol, and histone-H1 (2 μg/50 μl) at 30°C for 30 min, and the reaction was terminated by the addition of SDS–polyacrylamide gel electrophoresis (PAGE) sample buffer. After boiling for 5 min, the samples were subjected to SDS-PAGE. The gels were stained with Coomassie blue, dried, and exposed to x-ray film for autoradiography at −80°C.

GST pull-down assay

The GST or His-tagged protein purification and in vitro GST pull-down assays were performed as described previously (*20*). Thirty microliters of glutathione agarose beads (Protein A-Sepharose CL-4, Amersham Pharmacia) was incubated with 500 μg of proteins from cell lysate or mouse brain lysate mixed with GST or GST-tagged proteins in a total volume of 400 μl at 4°C overnight. The beads were washed six times with TBS with 0.1% Triton X-100, and the proteins were detected by Western blotting.

Ca^{2+} imaging

For Fluo-4 AM Ca^{2+} imaging, HEK293 cells transfected with GST-TRPV1 or primary cultured DRG neurons were loaded with 5 μM Fluo-4 AM (Invitrogen, USA) for 40 min at 37°C and then washed three times and left in Hanks' balanced salt solution (HBSS) without phenol red (GE Healthcare, USA). Cells were then transferred at 37°C to allow membrane protein internalization or 4°C for control for 15 min. After being balanced at room temperature for more than 30 min, cell images were acquired every 5 s with an inverted Leica TCS SP8 microscope (Germany) with an APO 25× objective (water, NA 0.95) and a 488-nm argon laser. The real-time fluorescence intensity was analyzed by Leica LAS X software.

For Fura-2 AM Ca^{2+} imaging, after application of TAT-S45 peptide or TAT-S45A peptide (10 μg) for 4 hours, HEK293 cells were subjected to Fura-2 AM-based Ca^{2+} imaging experiments as described previously (*19*). Cells were loaded with 5 μM Fura-2 AM (Biotium) for 30 min at 37°C and then washed three times and left in HBSS without phenol red (GE Healthcare). For Ca^{2+} imaging, an inverted fluorescent microscope equipped with a 340- and 380-nm excitation filter changer (Olympus) with MetaFluor software was used. The F_{340}/F_{380} ratio was acquired every 5 s. TRPV1 activation was evoked by the addition of 5 μM capsaicin. Cells that failed to respond to 25 mM KCl were discarded from the analysis. Cells derived from at least three separate isolations were analyzed.

Animals and behavioral experiments

Male Sprague-Dawley (SD) rats (200 to 250 g) from the Experimental Animal Center of Peking University were used. Animal experiments were all conducted according to the guidelines of the Animal Care and Use Committee of Peking University. Rats were housed in a specific pathogen–free laboratory animal room, with four to six rats per cage, under natural lighting and free access to water and food. Before the experiments, the rats were allowed to acclimate to the environment for at least 3 days.

Intrathecal injections were performed as described previously (*19*). Briefly, animals were anesthetized with 10% chloral hydrate (0.3 g/kg, i.p.), and a PE-10 polyethylene catheter was implanted into the intrathecal space to reach the lumbar enlargement of the spinal cord. After recovery for 4 to 5 days after the surgery, 10 μl of TAT peptide was intrathecally administered.

For spontaneous pain behavior test, capsaicin (0.5 mM, 30 μl) was injected intraplantarly into the left hind paw 30 min after intrathecal administration of TAT peptide. All intraplantar injections were performed via microsyringe (Hamilton) in awake SD rats, and the needle remained in situ for 10 s before withdrawal. After intraplantar injection of capsaicin, spontaneous pain behavior was tested by counting the total lifting time in the first 5 min.

For the CFA-induced model, TAT peptide was intrathecally administered 30 min before injection of 100 μl of 25% CFA (diluted with IFA) into the plantar surface of the left hind paw. Thermoalgesia was determined using a radiant heat stimulus and expressed as the PWL. The basal PWL after recovery of surgery was tested before drug administration. Heat hyperalgesia was assessed 1, 2, and 6 hours and 1 day after CFA injection. For the experiments designed to assess the effect of TAT-S45 peptide on the basal heat sensitivity, the same dose of TAT peptides was injected intrathecally, and the basal heat sensitivity was tested 1.5, 2.5, and 6.5 hours and 1 day after intrathecal injection.

Statistical analyses

Experiments and analysis were performed in a blinded manner. Data are expressed as the means ± SEM. Statistical analyses were performed using Prism 5.0 software (GraphPad Software Inc.). Differences between groups were compared using either *t* test or two-way ANOVA, followed by Bonferroni's post hoc tests. Statistical significance was set at $P < 0.05$ (*$P < 0.05$, **$P < 0.01$, ***$P < 0.001$). For Western blotting, the immunoreactive bands were scanned and analyzed quantitatively using Quantity One software (Bio-Rad Laboratories).

REFERENCES AND NOTES

1. D. E. Clapham, TRP channels as cellular sensors. *Nature* **426**, 517–524 (2003).
2. B. Nilius, TRP channels in disease. *Biochim. Biophys. Acta* **1772**, 805–812 (2007).

3. E. Palazzo, L. Luongo, V. de Novellis, L. Berrino, F. Rossi, S. Maione, Moving towards supraspinal TRPV1 receptors for chronic pain relief. *Mol. Pain* **6**, 66 (2010).
4. Y. Wang, The functional regulation of TRPV1 and its role in pain sensitization. *Neurochem. Res.* **33**, 2008–2012 (2008).
5. M. C. Lagerstrom, K. Rogoz, B. Abrahamsen, E. Persson, B. Reinius, K. Nordenankar, C. Olund, C. Smith, J. A. Mendez, Z.-F. Chen, J. N. Wood, A. Wallén-Mackenzie, K. Kullander, VGLUT2-dependent sensory neurons in the TRPV1 population regulate pain and itch. *Neuron* **68**, 529–542 (2010).
6. C. E. Riera, M. O. Huising, P. Follett, M. Leblanc, J. Halloran, R. Van Andel, C. D. de Magalhaes Filho, C. Merkwirth, A. Dillin, TRPV1 pain receptors regulate longevity and metabolism by neuropeptide signaling. *Cell* **157**, 1023–1036 (2014).
7. R. Razavi, Y. Chan, F. N. Afifiyan, X. J. Liu, X. Wan, J. Yantha, H. Tsui, L. Tang, S. Tsai, P. Santamaria, J. P. Driver, D. Serreze, M. W. Salter, H.-M. Dosch, TRPV1^{+} sensory neurons control β cell stress and islet inflammation in autoimmune diabetes. *Cell* **127**, 1123–1135 (2006).
8. J. M. Romac, S. J. McCall, J. E. Humphrey, J. Heo, R. A. Liddle, Pharmacologic disruption of TRPV1-expressing primary sensory neurons but not genetic deletion of TRPV1 protects mice against pancreatitis. *Pancreas* **36**, 394–401 (2008).
9. S. J. Ives, S. Y. Park, O. S. Kwon, J. R. Gifford, R. H. I. Andtbacka, J. R. Hyngstrom, R. S. Richardson, $TRPV_1$ channels in human skeletal muscle feed arteries: Implications for vascular function. *Exp. Physiol.* **102**, 1245–1258 (2017).
10. J. Lee, M.-K. Chung, J. Y. Ro, Activation of NMDA receptors leads to phosphorylation of TRPV1 S800 by protein kinase C and A-kinase anchoring protein 150 in rat trigeminal ganglia. *Biochem. Biophys. Res. Commun.* **424**, 358–363 (2012).
11. E. D. Por, R. Gomez, A. N. Akopian, N. A. Jeske, Phosphorylation regulates TRPV1 association with β-arrestin-2. *Biochem. J.* **451**, 101–109 (2013).
12. L. Li, R. Hasan, X. Zhang, The basal thermal sensitivity of the TRPV1 ion channel is determined by PKCβII. *J. Neurosci.* **34**, 8246–8258 (2014).
13. L. Duo, L. Hu, N. Tian, G. Cheng, H. Wang, Z. Lin, Y. Wang, Y. Yang, TRPV1 gain-of-function mutation impairs pain and itch sensations in mice. *Mol. Pain* **14**, 1744806918762031 (2018).
14. H. Zhu, Y. Yang, H. Zhang, Y. Han, Y. Li, Y. Zhang, D. Yin, Q. He, Z. Zhao, P. M. Blumberg, J. Han, Y. Wang, Interaction between protein kinase D1 and transient receptor potential V1 in primary sensory neurons is involved in heat hypersensitivity. *Pain* **137**, 574–588 (2008).
15. S. Laínez, P. Valente, I. Ontoria-Oviedo, J. Estévez-Herrera, M. Camprubí-Robles, A. Ferrer-Montiel, R. Planells-Cases, $GABA_A$ receptor associated protein (GABARAP) modulates TRPV1 expression and channel function and desensitization. *FASEB J.* **24**, 1958–1970 (2010).
16. L. Sanz-Salvador, A. Andrés-Borderia, A. Ferrer-Montiel, R. Planells-Cases, Agonist- and Ca^{2+}-dependent desensitization of TRPV1 channel targets the receptor to lysosomes for degradation. *J. Biol. Chem.* **287**, 19462–19471 (2012).
17. F. Mori, M. Ribolsi, H. Kusayanagi, F. Monteleone, V. Mantovani, F. Buttari, E. Marasco, G. Bernardi, M. Maccarrone, D. Centonze, TRPV1 channels regulate cortical excitability in humans. *J. Neurosci.* **32**, 873–879 (2012).
18. A. Mandal, M. Shahidullah, N. A. Delamere, TRPV1-dependent ERK1/2 activation in porcine lens epithelium. *Exp. Eye Res.* **172**, 128–136 (2018).
19. J. Liu, J. Du, Y. Yang, Y. Wang, Phosphorylation of TRPV1 by cyclin-dependent kinase 5 promotes TRPV1 surface localization, leading to inflammatory thermal hyperalgesia. *Exp. Neurol.* **273**, 253–262 (2015).
20. B.-M. Xing, Y.-R. Yang, J.-X. Du, H.-J. Chen, C. Qi, Z.-H. Huang, Y. Zhang, Y. Wang, Cyclin-dependent kinase 5 controls TRPV1 membrane trafficking and the heat sensitivity of nociceptors through KIF13B. *J. Neurosci.* **32**, 14709–14721 (2012).
21. B. T. Kelly, S. C. Graham, N. Liska, P. N. Dannhauser, S. Höning, E. J. Ungewickell, D. J. Owen, AP2 controls clathrin polymerization with a membrane-activated switch. *Science* **345**, 459–463 (2014).
22. B. T. Kelly, A. J. McCoy, K. Späte, S. E. Miller, P. R. Evans, S. Höning, D. J. Owen, A structural explanation for the binding of endocytic dileucine motifs by the AP2 complex. *Nature* **456**, 976–979 (2008).
23. L. A. Wood, G. Larocque, N. I. Clarke, S. Sarkar, S. J. Royle, New tools for "hot-wiring" clathrin-mediated endocytosis with temporal and spatial precision. *J. Cell Biol.* **216**, 4351–4365 (2017).
24. G. Fattakhova, M. Masilamani, F. Borrego, A. M. Gilfillan, D. D. Metcalfe, J. E. Coligan, The high-affinity immunoglobulin-E receptor (FcepsilonRI) is endocytosed by an AP-2/clathrin-independent, dynamin-dependent mechanism. *Traffic* **7**, 673–685 (2006).
25. E. Cocucci, R. Gaudin, T. Kirchhausen, Dynamin recruitment and membrane scission at the neck of a clathrin-coated pit. *Mol. Biol. Cell* **25**, 3595–3609 (2014).
26. K. Sandvig, S. Pust, T. Skotland, B. van Deurs, Clathrin-independent endocytosis: Mechanisms and function. *Curr. Opin. Cell Biol.* **23**, 413–420 (2011).
27. S. Holland, O. Coste, D. D. Zhang, S. C. Pierre, G. Geisslinger, K. Scholich, The ubiquitin ligase MYCBP2 regulates transient receptor potential vanilloid receptor 1 (TRPV1) internalization through inhibition of p38 MAPK signaling. *J. Biol. Chem.* **286**, 3671–3680 (2011).
28. R. Planells-Cases, A. Ferrer-Montiel, in *TRP Ion Channel Function in Sensory Transduction and Cellular Signaling Cascades*, W. B. Liedtke, S. Heller, Eds. (CRC Press/Taylor & Francis, 2007), Chapter 23.
29. S. E. Jacobsen, I. Ammendrup-Johnsen, A. M. Jansen, U. Gether, K. L. Madsen, H. Bräuner-Osborne, The GPRC6A receptor displays constitutive internalization and sorting to the slow recycling pathway. *J. Biol. Chem.* **292**, 6910–6926 (2017).
30. H. T. McMahon, E. Boucrot, Molecular mechanism and physiological functions of clathrin-mediated endocytosis. *Nat. Rev. Mol. Cell Biol.* **12**, 517–533 (2011).
31. S. F. J. van de Graaf, U. Rescher, J. G. J. Hoenderop, S. Verkaart, R. J. M. Bindels, V. Gerke, TRPV5 is internalized via clathrin-dependent endocytosis to enter a Ca^{2+}-controlled recycling pathway. *J. Biol. Chem.* **283**, 4077–4086 (2008).
32. W.-Z. Zeng, D.-S. Liu, B. Duan, X.-L. Song, X. Wang, D. Wei, W. Jiang, M. X. Zhu, Y. Li, T.-L. Xu, Molecular mechanism of constitutive endocytosis of acid-sensing ion channel 1a and its protective function in acidosis-induced neuronal death. *J. Neurosci.* **33**, 7066–7078 (2013).
33. H. Damke, D. D. Binns, H. Ueda, S. L. Schmid, T. Baba, Dynamin GTPase domain mutants block endocytic vesicle formation at morphologically distinct stages. *Mol. Biol. Cell* **12**, 2578–2589 (2001).
34. D. J. Owen, B. M. Collins, P. R. Evans, Adaptors for clathrin coats: Structure and function. *Annu. Rev. Cell Dev. Biol.* **20**, 153–191 (2004).
35. W.-Y. Xie, Y. He, Y.-R. Yang, Y.-F. Li, K. Kang, B.-M. Xing, Y. Wang, Disruption of Cdk5-associated phosphorylation of residue threonine-161 of the δ-opioid receptor: Impaired receptor function and attenuated morphine antinociceptive tolerance. *J. Neurosci.* **29**, 3551–3564 (2009).
36. T. K. Pareek, J. Keller, S. Kesavapany, N. Agarwal, R. Kuner, H. C. Pant, M. J. Iadarola, R. O. Brady, A. B. Kulkarni, Cyclin-dependent kinase 5 modulates nociceptive signaling through direct phosphorylation of transient receptor potential vanilloid 1. *Proc. Natl. Acad. Sci. U.S.A.* **104**, 660–665 (2007).
37. R.-R. Ji, T. A. Samad, S.-X. Jin, R. Schmoll, C. J. Woolf, p38 MAPK activation by NGF in primary sensory neurons after inflammation increases TRPV1 levels and maintains heat hyperalgesia. *Neuron* **36**, 57–68 (2002).
38. S. Han, S. M. Kang, J.-H. Oh, D. H. Lee, J. H. Chung, Src kinase mediates UV-induced TRPV1 trafficking into cell membrane in HaCaT keratinocytes. *Photodermatol. Photoimmunol. Photomed.* **34**, 214–216 (2018).
39. H. Gao, K. Miyata, M. D. Bhaskaran, A. V. Derbenev, A. Zsombok, Transient receptor potential vanilloid type 1-dependent regulation of liver-related neurons in the paraventricular nucleus of the hypothalamus diminished in the type 1 diabetic mouse. *Diabetes* **61**, 1381–1390 (2012).
40. M. E. Johansen, C. A. Reilly, G. S. Yost, TRPV1 antagonists elevate cell surface populations of receptor protein and exacerbate TRPV1-mediated toxicities in human lung epithelial cells. *Toxicol. Sci.* **89**, 278–286 (2006).
41. Y. R. Yang, Y. He, Y. Zhang, Y. Li, Y. Li, Y. Han, H. Zhu, Y. Wang, Activation of cyclin-dependent kinase 5 (Cdk5) in primary sensory and dorsal horn neurons by peripheral inflammation contributes to heat hyperalgesia. *Pain* **127**, 109–120 (2007).
42. F. A. Dhariwala, M. S. Rajadhyaksha, An unusual member of the Cdk family: Cdk5. *Cell. Mol. Neurobiol.* **28**, 351–369 (2008).
43. C. Coddou, R. Sandoval, P. Castro, P. Lazcano, M. J. Hevia, M. Rokic, B. Hall, A. Terse, C. Gonzalez-Billault, A. B. Kulkarni, S. S. Stojilkovic, E. Utreras, Cyclin-dependent kinase 5 modulates the P2X2a receptor channel gating through phosphorylation of C-terminal threonine 372. *Pain* **158**, 2155–2168 (2017).
44. Z.-Y. Zhuang, H. Xu, D. E. Clapham, R.-R. Ji, Phosphatidylinositol 3-kinase activates ERK in primary sensory neurons and mediates inflammatory heat hyperalgesia through TRPV1 sensitization. *J. Neurosci.* **24**, 8300–8309 (2004).
45. X. Zhang, J. Huang, P. A. McNaughton, NGF rapidly increases membrane expression of TRPV1 heat-gated ion channels. *EMBO J.* **24**, 4211–4223 (2005).
46. Y. Sugimoto, Y. Kojima, A. Inayoshi, K. Inoue, H. Miura-Kusaka, K. Mori, O. Saku, H. Ishida, E. Atsumi, Y. Nakasato, S. Shirakura, S. Toki, K. Shinoda, N. Suzuki, K-685, a TRPV1 antagonist, blocks PKC-sensitized TRPV1 activation and improves the inflammatory pain in a rat complete Freund's adjuvant model. *J. Pharmacol. Sci.* **123**, 256–266 (2013).
47. M. Nakanishi, K. Hata, T. Nagayama, T. Sakurai, T. Nishisho, H. Wakabayashi, T. Hiraga, S. Ebisu, T. Yoneda, Acid activation of Trpv1 leads to an up-regulation of calcitonin gene-related peptide expression in dorsal root ganglion neurons via the CaMK-CREB cascade: A potential mechanism of inflammatory pain. *Mol. Biol. Cell* **21**, 2568–2577 (2010).
48. J.-D. Brederson, P. R. Kym, A. Szallasi, Targeting TRP channels for pain relief. *Eur. J. Pharmacol.* **716**, 61–76 (2013).
49. D. Feingold, S. Brill, I. Goor-Aryeh, Y. Delayahu, S. Lev-Ran, Misuse of prescription opioids among chronic pain patients suffering from anxiety: A cross-sectional analysis. *Gen. Hosp. Psychiatry* **47**, 36–42 (2017).
50. F. Gedin, M. Skeppholm, K. Burstrom, V. Sparring, M. Tessma, N. Zethraeus, Effectiveness, costs and cost-effectiveness of chiropractic care and physiotherapy compared with information and advice in the treatment of non-specific chronic low back pain: Study protocol for a randomised controlled trial. *Trials* **18**, 613 (2017).

51. E. Dragioti, L. Bernfort, B. Larsson, B. Gerdle, L. Å. Levin, Association of insomnia severity with well-being, quality of life and health care costs: A cross-sectional study in older adults with chronic pain (PainS65+). *Eur. J. Pain* **22**, 414–425 (2018).
52. T. E. Dorner, Pain and chronic pain epidemiology: Implications for clinical and public health fields. *Wien. Klin. Wochenschr.* **130**, 1–3 (2018).
53. G. J. Macfarlane, The epidemiology of chronic pain. *Pain* **157**, 2158–2159 (2016).
54. P. Knaster, H. Karlsson, A.-M. Estlander, E. Kalso, Psychiatric disorders as assessed with SCID in chronic pain patients: The anxiety disorders precede the onset of pain. *Gen. Hosp. Psychiatry* **34**, 46–52 (2012).
55. T. Mainka, N. M. Malewicz, R. Baron, E. K. Enax-Krumova, R.-D. Treede, C. Maier, Presence of hyperalgesia predicts analgesic efficacy of topically applied capsaicin 8% in patients with peripheral neuropathic pain. *Eur. J. Pain* **20**, 116–129 (2016).
56. Ottawa, *Long-acting Opioids for Chronic Non-cancer Pain: A Review of the Clinical Efficacy and Safety* (Canadian Agency for Drugs and Technologies in Health, 2015).
57. Y. Wang, N. Kedei, M. Wang, Q. J. Wang, A. R. Huppler, A. Toth, R. Tran, P. M. Blumberg, Interaction between protein kinase Cμ and the vanilloid receptor type 1. *J. Biol. Chem.* **279**, 53674–53682 (2004).

Funding: This work was supported by grants from the National Natural Science Foundation of China (31720103908 and 31530028 to Y.W., 31700898 to J.L., and 81821092 to J.L.) and the National Key Technology Support Program of the Ministry of Science and Technology of China (973 program: 2017YFA0701302 to Y.W.). **Author contributions:** Y.W., J.L., and J.D. designed the experiments; J.L. and J.D. performed the experiments; and Y.W. and J.L. wrote the paper. **Competing interests:** The authors declare that they have no competing financial interests. **Data and materials availability:** All data needed to evaluate the conclusions in the paper are present in the paper.

Submitted 28 November 2018
Accepted 17 May 2019
Published 11 June 2019
10.1126/scisignal.aaw2040

Citation: J. Liu, J. Du, Y. Wang, CDK5 inhibits the clathrin-dependent internalization of TRPV1 by phosphorylating the clathrin adaptor protein AP2μ2. *Sci. Signal.* **12**, eaaw2040 (2019).

Science Signaling

CDK5 inhibits the clathrin-dependent internalization of TRPV1 by phosphorylating the clathrin adaptor protein AP2 μ2

Jiao Liu, Junxia Du and Yun Wang

Sci. Signal. **12** (585), eaaw2040.
DOI: 10.1126/scisignal.aaw2040

Constitutive internalization of a nociceptor

The nonselective cation channel TRPV1 elicits the sensation of burning pain in response to thermal or chemical stimuli and contributes to inflammatory thermal hyperalgesia, the increased sensitivity of inflamed tissues to heat. Liu *et al* . found that TRPV1 was constitutively internalized in cultured human cells and rat neurons through clathrin-mediated endocytosis. TRPV1 internalization depended on binding to the clathrin adaptor protein complex 2 subunit μ2 (AP2μ2) and was antagonized by phosphorylation of AP2 μ2 by cyclin-dependent kinase 5 (CDK5). Treating rats with a peptide that interfered with Cdk5-mediated AP2 μ2 phosphorylation reduced inflammatory thermal hyperalgesia, suggesting that strategies for promoting TRPV1 internalization might lead to effective treatments for pain.